

ADA021168

12
NW

Determination of Graphite-Liquid-Vapor Triple Point by Laser Heating

N. A. GOKCEN, E. T. CHANG, and T. M. POSTON
Chemistry and Physics Laboratory

and

D. J. SPENCER
Aerophysics Laboratory ✓
Laboratory Operations
The Aerospace Corporation
El Segundo, Calif. 90245

30 January 1976

Interim Report

APPROVED FOR PUBLIC RELEASE:
DISTRIBUTION UNLIMITED

DDC
RECEIVED
FEB 26 1976
D

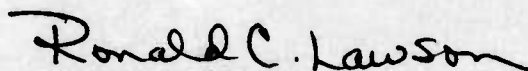
Prepared for
SPACE AND MISSILE SYSTEMS ORGANIZATION
AIR FORCE SYSTEMS COMMAND
Los Angeles Air Force Station
P.O. Box 92960, Worldway Postal Center
Los Angeles, Calif. 90009

This report was submitted by The Aerospace Corporation, El Segundo, CA 90245, under Contract F04701-75-C-0076 with the Space and Missile Systems Organization, Deputy for Advanced Space Programs, P.O. Box 92960, Worldway Postal Center, Los Angeles, CA 90009. It was reviewed and approved for The Aerospace Corporation by S. Siegel, Director, Chemistry and Physics Laboratory, and W. R. Warren, Jr., Director, Aerophysics Laboratory. Lt. Ronald C. Lawson, SAMSO/DYN, was the project officer.

This report has been reviewed by the Information Office (OI) and is releasable to the National Technical Information Service (NTIS). At NTIS, it will be available to the general public, including foreign nations.

This technical report has been reviewed and is approved for publication. Publication of this report does not constitute Air Force approval of the report's findings or conclusions. It is published only for the exchange and stimulation of ideas.

FOR THE COMMANDER



Ronald C. Lawson, 2nd Lt., USAF
Office of Research Application
Deputy for Technology

UNCLASSIFIED

SECURITY CLASSIFICATION OF THIS PAGE (When Data Entered)

19 REPORT DOCUMENTATION PAGE		READ INSTRUCTIONS BEFORE COMPLETING FORM	
1. REPORT NUMBER 18 SAMS0-TR-76-29 ✓	2. GOVT ACCESSION NO.	3. RECIPIENT'S CATALOG NUMBER	
4. TITLE (and Subtitle) 6 DETERMINATION OF GRAPHITE-LIQUID-VAPOR TRIPLE POINT BY LASER HEATING		5. TYPE OF REPORT & PERIOD COVERED 9 Interim rept.	
7. AUTHOR(s) 10 N. A. Gokcen, E. T. Chang, T. M. Poston, and D. J. Spencer		6. PERFORMING ORG. REPORT NUMBER 14 TR-0076(6270-10)-1 ✓	
9. PERFORMING ORGANIZATION NAME AND ADDRESS The Aerospace Corporation ✓ El Segundo, Calif. 90245		8. CONTRACT OR GRANT NUMBER(s) 15 F04701-75-C-0076	
11. CONTROLLING OFFICE NAME AND ADDRESS Space and Missile Systems Organization Air Force Systems Command Los Angeles, Calif. 90009		10. PROGRAM ELEMENT, PROJECT, TASK AREA & WORK UNIT NUMBERS 12 60P.	
14. MONITORING AGENCY NAME & ADDRESS (if different from Controlling Office)		12. REPORT DATE 11 30 January 1976	
		13. NUMBER OF PAGES 56	
		15. SECURITY CLASS. (of this report) Unclassified	
		15a. DECLASSIFICATION/DOWNGRADING SCHEDULE	
16. DISTRIBUTION STATEMENT (of this Report) Approved for public release; distribution unlimited			
17. DISTRIBUTION STATEMENT (of the abstract entered in Block 20, if different from Report) D D C RECEIVED FEB 26 1976 RECEIVED D			
18. SUPPLEMENTARY NOTES			
19. KEY WORDS (Continue on reverse side if necessary and identify by block number) Graphite, graphite structure, HF laser, phase diagram, triple point, vapor pressure			
20. ABSTRACT (Continue on reverse side if necessary and identify by block number) A technique was developed for measuring the melting temperatures of graphite, and the graphite-liquid-vapor triple point by means of continuous HF laser in the pressure range 120 to 215 atm. The triple point was found to be 120 ± 10 atm and 4130 ± 30 K for pyrolytic graphite. The results with neon, argon, and krypton as pressurization gases were concordant. A vapor-solid-liquid phase diagram was obtained in the vicinity of triple point.			

DD FORM 1473
(FACSIMILE)

+ 01 -

UNCLASSIFIED

SECURITY CLASSIFICATION OF THIS PAGE (When Data Entered)

UNCLASSIFIED

SECURITY CLASSIFICATION OF THIS PAGE(When Data Entered)

19. KEY WORDS (Continued)

20. ABSTRACT (Continued)

Photomicrography, electron micrography, x-ray diffraction, and ion microprobe mass analysis were used to characterize the structure of frozen liquid droplets, the pyrolytic graphite matrix, and condensed vapor.

UNCLASSIFIED

SECURITY CLASSIFICATION OF THIS PAGE(When Data Entered)

PREFACE

The authors are indebted to Dr. W. R. Warren, Jr., for his encouragement, Dr. G. M. Wolten for x-ray analyses, and Dr. W. K. Stuckey for ion microprobe mass analyses. Mr. T. J. Bertone polished and photomicrographed various samples and Ms. A. L. Palyo obtained the SEM micrographs. Messrs. H. A. Bixler, T. L. Felker, and J. M. Blades operated and controlled the HF laser.

ACCESSION for		
DTIS	White Section	<input checked="" type="checkbox"/>
DDC	Buff Section	<input type="checkbox"/>
UNANNOUNCED		<input type="checkbox"/>
JUSTIFICATION.....		
BY		
DISTRIBUTION/AVAILABILITY CODES		
Dist.	AVAIL. and/or SPECIAL	
A		

D D C

RECEIVED

FEB 26 1976

D

CONTENTS

PREFACE	1
I. INTRODUCTION	7
II. EXPERIMENTAL PROCEDURE	19
A. Phase Equilibria Results	22
B. Microstructure	22
C. X-Ray and Ion Microprobe Mass Analyses	50
III. DISCUSSIONS	53
A. Triple-Point Pressure	53
B. Triple-Point Temperature	54
C. Phase Diagram	55
IV. SUMMARY	57
REFERENCES	59

FIGURES

1.	Graphite specimen used by Schoessow for resistance heating	10
2.	Steady-state temperature vs laser power for pyrolytic graphite at 1.0-Torr chamber pressure	13
3.	Carbon vapor pressure vs temperature	14
4.	Equilibrium pressure P_3 of $C_3(g)$ over solid and liquid carbon	15
5.	Apparatus	20
6.	Graphite-liquid-vapor triple point and melting temperatures of graphite	23
7.	Sample No. 152 at 4140 K and 146 atm of neon.	24
8.	Same as Figure 7	25
9.	Sample No. 140 at 4180 K and 143 atm of neon	26
10.	Same as Figure 9	27
11.	Sample No. 11 at 4475 K and 160 atm of neon	29
12.	Cross section of Sample No. 11	30
13.	Same as Figure 12	31
14.	For caption, see Figure 18	32
15.	For caption, see Figure 18	33
16.	For caption, see Figure 18	34
17.	For caption, see Figure 18	35
18.	Cross section of Sample No. 11 under polarized light at various angles	36
19.	Sample No. 11, frozen droplet, cross-polarized light red-sensitive tint	37

FIGURES (Continued)

20.	Sample No. 11 (edge of crater showing condensate under cross-polarized light	38
21.	Sample No. 32 at 4005 K and 210 atm of neon	39
22.	For caption, see Figure 25	40
23.	For caption, see Figure 25	41
24.	For caption, see Figure 25	42
25.	Sample No. 32 showing no liquid	43
26.	Sample No. 38 at 4120 K and 193 atm of krypton	44
27.	Same as Figure 26 (Upper central part of crater)	45
28.	Central part of Figure 26 just below crack	46
29.	Outer edge of crater in Figure 26	47
30.	For caption, see Figure 31	48
31.	View of Sample No. 38 from right side of Figure 29 to central crack in Figure 27	49

I. INTRODUCTION

Graphite is an excellent ablator in extreme thermal and pressure environments encountered by missiles and reentry vehicles. Reliable data on the triple point and the melting temperatures and pressures are needed for calculating flight performance for the successful reentry of space vehicles. Such data are also useful for evaluating the optimum specific impulse of graphite nuclear propulsion reactors.

Experimental measurements become increasingly difficult with increasing temperatures beyond 2500 K because of the nonuniformity in heating and the inaccuracies in the equilibrium pressure and temperature measurements. Unusual experimental techniques have therefore been devised for measuring the triple point of graphite. The earliest systematic experiments for this purpose were carried out by Basset (Ref. 1). He used a power supply of 300 A and 12 to 30 V for resistance-heating a graphite rod with a reduced section 2 mm in diameter and 6 mm long. The graphite bar was pressurized with argon in a sealed chamber with an optical port for temperature measurements. Convection currents caused difficulties in the temperature measurements, which were made with an optical pyrometer. He considered that the failure of graphite rod was caused by the melting of graphite when the pressure was sufficiently high. The failure by melting was recorded by photographing the bar. Post-heating examination revealed shiny droplets of frozen liquid. At pressures below 100 atm, the graphite bars ruptured without forming droplets of graphite. On the basis of experiments at various pressures, Basset reported that the triple point of graphite is 102 atm and 4000 K.

Similar experiments by electric heating in a pressurized chamber were carried out by Jones (Ref. 2). He used a rectangular specimen 3.2×5.1 mm in cross section and 15.9 mm long with a shallow hole in the midpoint for optical temperature measurements. His results for the triple point, 100 atm and 4030 K, are in excellent agreement with those of Basset. Noda (Ref. 3) used a procedure nearly identical with that of Basset. He used a bar 4 mm in

diameter and 30 mm long but with a smaller diameter central section. Argon was used for pressurization. The temperature measurements were made with a calibrated optical pyrometer. Spherical shiny frozen droplets of graphite, 1 to 3 mm in diameter, indicated the occurrence of melting. The triple point obtained by Noda was 100 to 110 atm and 4020 ± 50 K, which is in agreement with the results of the similar experiments of Basset and Jones.

Bundy (Ref. 4) determined the melting points of graphite at high pressures by pulse-heating a bar of graphite 1 mm in diameter. The heating was accomplished by discharging a battery of capacitors. He used the energy balance and the extrapolated values of heat capacity to calculate the final temperature obtained in graphite. His results showed that the melting point of graphite increases with pressure to 4600 K at about 65,000 atm, with Basset's triple point used as the initial reference point. Bundy did not determine the actual triple point in these experiments.

Fateeva, Vereschagin, and Kolotygin (Ref. 5) electrically heated a spectrographically pure bar of graphite only 0.8 mm in diameter and 10 mm long in argon until failure by rupture occurred. They measured the temperature with a two-color pyrometer. The melting temperature in their experiments was reported as 4650 K at 3000 atm. Vereshchagin and Fateeva (Ref. 6) utilized the same apparatus and procedure but improved temperature measurements by using a three-color pyrometer. The results for the triple point were 4040 K and 100 atm. The melting point of graphite increased with pressure to 4090 K at 3000 atm and to 5000 K at 60,000 atm. At pressures in excess of 2000 atm, the sample was pressurized in NaCl, a medium that interfered with accurate temperature measurements because discoloration occurred. A substantial correction was therefore necessary for the optical temperature measured through NaCl. Fateeva and Vereshchagin (Ref. 7) revised their earlier data and obtained additional data up to 90,000 atm for the melting points of graphite. Their results for the triple point remained the same, but the melting point at 60,000 atm was reduced by 100 K to 4900 K.

Schoessow (Ref. 8) used up to 20 V and 3000 A to heat various grades of graphite pressurized with helium in a chamber. A bar of graphite slightly reduced to 10.9 mm in diameter in the midsection and 3.2 mm long was drilled along its axis to provide a vertical chimney for sweeping away graphite vapor and soot when it was positioned vertically for heating (Fig. 1). A 2-mm radial hole located in the center and terminating on the axial hole provided an optical tunnel for measuring temperature by means of a disappearing-filament optical pyrometer. In addition to the direct temperature measurements, indirect temperature measurements were obtained from the master curves, correlating the temperature versus the electric power input. For this purpose, simultaneous readings of temperature and power-input were obtained in the range where the interference from soot and vapor was negligible. The curve was extrapolated a few hundred degrees above the last simultaneous temperature-power reading; the power reading when melting occurred was subsequently used on the plot to obtain the melting temperature. The graphite bar melted at the axial center when the pressure was sufficiently high, but the outside surface remained solid. The beginning of melting was indicated by a rapid rise in voltage across the specimen. The bar was then cooled and examined under a microscope at 120 \times for frozen liquid droplets and a dendritic melted region to assure that melting had occurred. The frozen droplets were shiny in appearance and distinct in structure from the remaining portions of graphite. The bars heated below the triple-point pressure did not contain liquid droplets. The various grades of graphite used in his experiments melted at or above 103 atm, which was the triple-point pressure in these experiments. The triple-point temperature, however, ranged from 4180 to 4300 K. The 4300 K temperature was for the spectroscopic grade graphite (AGKS, Union Carbide Corporation). An increase in pressure from 100 to 1000 atm caused a corresponding increase of 59 K in the melting point of graphite.

Dipconis, Stover, Hook, and Catalano (Ref. 9) used graphite bars similar to those used by Schoessow but with a graphite radiation shield heated separately to minimize the radiative heat loss from the bar. The pyrolytic

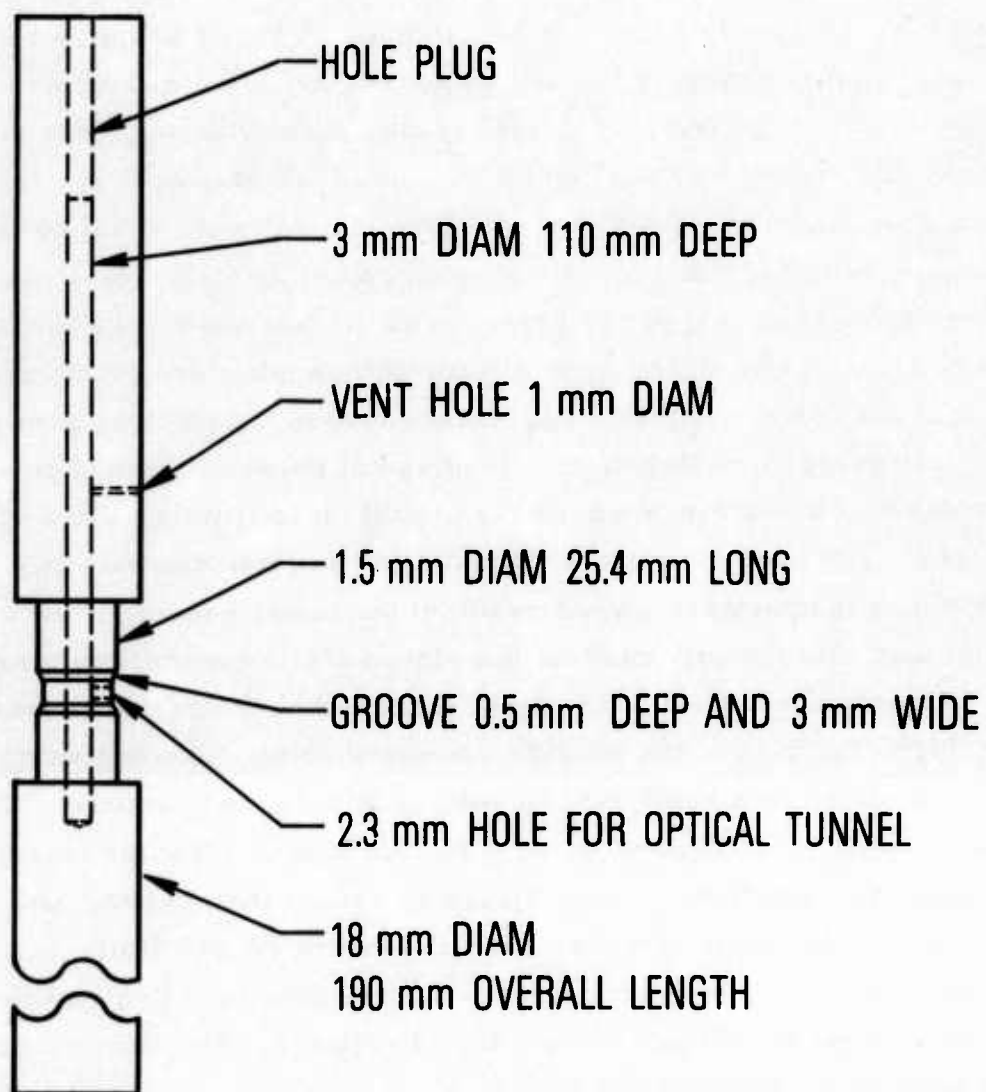


Fig. 1. Graphite specimen used by Schoessow for resistance heating

graphite bars used in their experiments contained 0.002% ash; the ATJ graphite bars, 0.044% ash. The results were concordant when either argon or nitrogen was used for pressurization. The temperature measurements were made by means of a recording optical pyrometer focused on a cavity on the graphite bar. The specimen was held horizontally, and the temperature was measured through a vertical port from the bottom of the chamber. The triple point of graphite was found to be 4100 to 4300 K and 103 atm. Frozen droplets of graphite were micrographically examined to reveal a crystalline structure distinctly different from the unmelted graphite matrix. The top surfaces of the frozen droplets were shiny and quite different from the dull unmelted graphite.

Diaconis et al. (Ref. 9) also determined the triple-point temperature by means of the direct arc-column radiation heating of a horizontal surface of graphite in argon or nitrogen. The disturbance of the surface gas layer by the arc made the measurement of the triple-point pressure difficult, but at pressures above 135 atm, it was possible to obtain droplets and rivulets of graphite. The surface temperature in these experiments were read with a scanning spectrometer. Significant temperature corrections, due to the emissivities of pyrolytic and ATJ graphite, were made to obtain melting temperatures in agreement with those obtained by resistive heating of graphite bars. The droplets obtained in these experiments exhibited the same appearance and microstructure as those from the graphite bars. Earlier experiments with arc-heating, summarized by Palmer and Shelef (Ref. 10), produced inconclusive results on the triple point.

Whittaker, Kintner, Nelson, and Richardson (Ref. 11) used a 6-kW continuous CO₂ laser beam to heat rapidly spinning pyrolytic graphite bars in a pressurized chamber. The power density was 47 kW cm⁻². A single experiment usually lasted 4 sec; during which time, the temperature measurements were made by means of two recording pyrometers 30 and 150 deg from the laser beam. A high-speed cinematograph was used to record the experiment. It was observed that for a selected pressure, in the range of 0.0016 to 6 atm, the curve for temperature versus time reached a steady value of temperature

even when the laser power was increased steadily as a function of time. They claimed that "This result (steady temperature) indicates that the carbon vapor is in pressure equilibrium with the chamber gas." When the laser power was increased beyond the start of the steady temperature, the carbon vapor pressure became greater than the chamber pressure and the carbon gas expanded away from the graphite bar and carried with it the excess laser power. The steady-state temperatures for various pressures were then plotted versus the laser power for a pressure range of 0.0016 to 6 atm (Fig. 2). Although the points were connected by three straight lines, it is evident that within the usual scattering encountered in high-temperature research it is justifiable to draw a continuous curve satisfying these points. In Fig. 2, as drawn, the first break was taken to be the sublimation point, and the second break, the triple point. The triple point was claimed to be 3780 ± 30 K and 0.19 ± 0.02 atm. The equilibrium total pressure was plotted versus temperature T , in K, as reproduced in Fig. 3 to claim that a sharp break in the vapor pressure occurred at the triple point. This figure was used by the present authors to obtain a plot of $\ln P_3$ of the dominant triatomic gaseous species versus T^{-1} as shown in Fig. 4. Since the total pressure shown by Whittaker et al. in Fig. 3 is lower than that from the JANAF Thermochemical Tables (Ref. 12), except at 3780 K, P_3 had to be calculated from the total pressure in Fig. 3 by using the gas-phase equilibrium constants for four dominant gaseous species in the JANAF tables. This procedure is justified because the gas phase was assumed to be in equilibrium either with the liquid phase or the solid phase, depending on temperature. From the slopes of the lines in Fig. 4, the following computations were made, where $\Delta H_{\text{vap}}^{\circ}$, $\Delta H_{\text{subl}}^{\circ}$, and $\Delta H_{\text{m}}^{\circ}$ are the standard molar enthalpies of vaporization, sublimation, and melting, respectively, and $\Delta S_{\text{m}}^{\circ}$ is the standard entropy of melting:

$$\text{Slope} = \frac{\partial \ln P_3}{\partial (1/T)} = - \frac{\Delta H^{\circ}(\text{vap or subl})}{R} \quad (1)$$

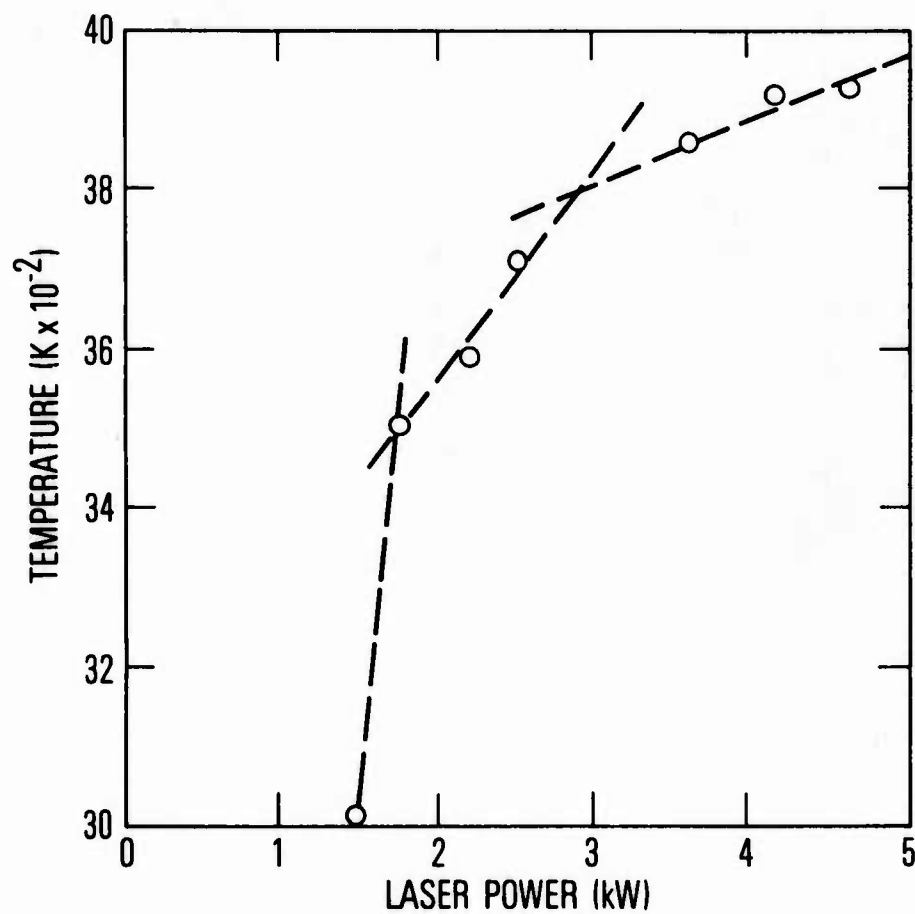


Fig. 2. Steady-state temperature vs laser power for pyrolytic graphite at 1.0-Torr chamber pressure. (From Whittaker et al.)

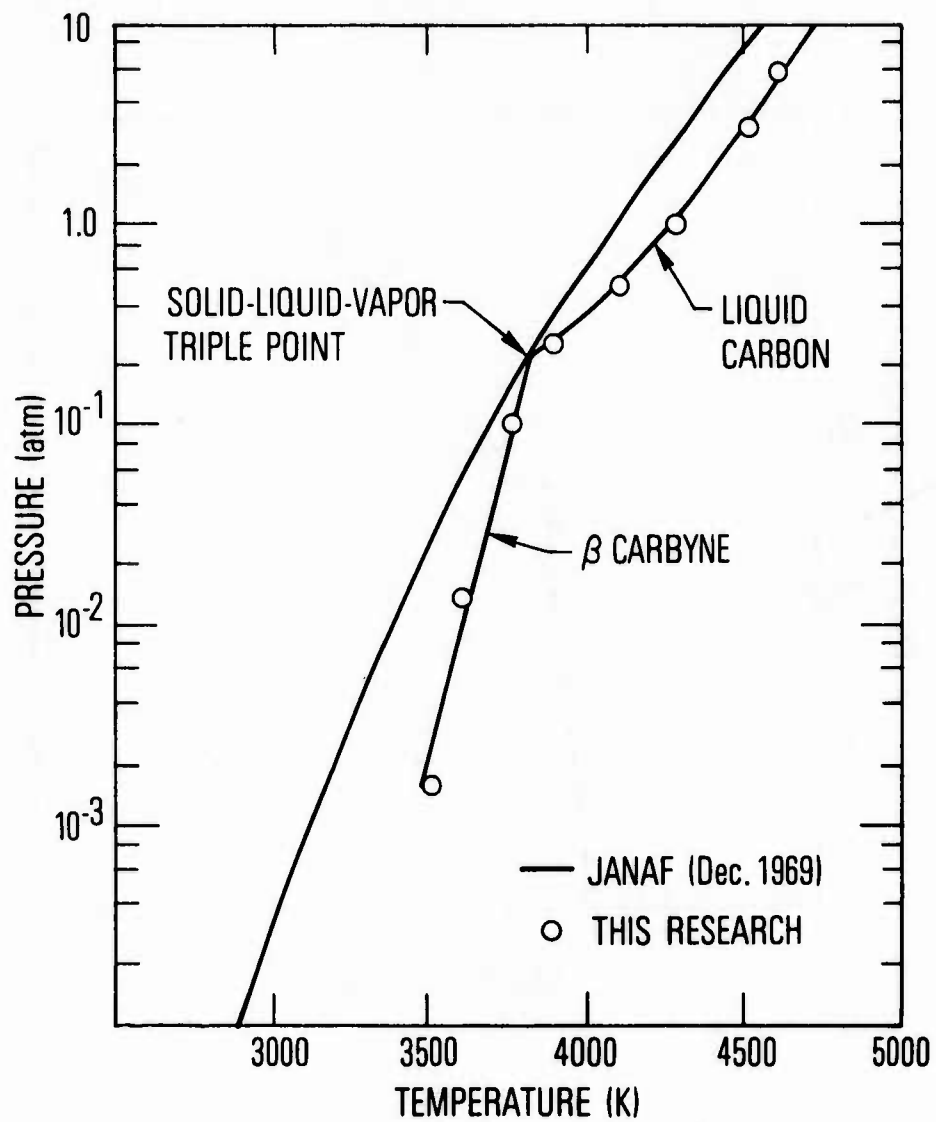


Fig. 3. Carbon vapor pressure vs temperature.
(From Whittaker et al.)

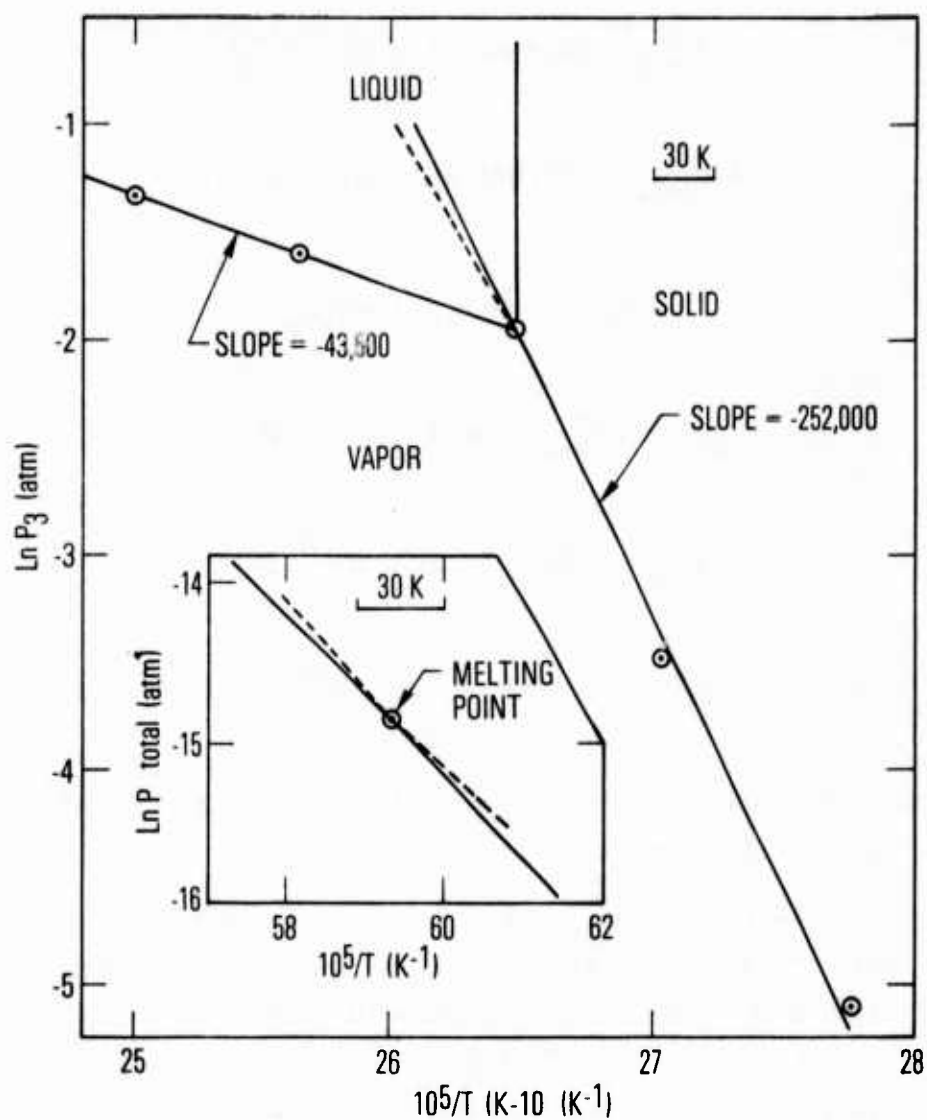


Fig. 4. Equilibrium pressure P_3 of $C_3(g)$ over solid and liquid carbon. (From Whittaker et al.) (Circles are from smooth curve in Fig. 3. Broken line in liquid region is for P_3 over liquid for entropy of melting corresponding to $\Delta S_m = 5.7 \text{ cal mole}^{-1} \text{ K}^{-1}$. Insert shows $\ln P$ vs $10^5/T$ for silicon.)

$$\Delta H_{\text{vap}}^{\circ} = 86,400 \text{ cal mole}^{-1} (\text{C}_3) \quad (2)$$

$$\Delta H_{\text{subl}}^{\circ} = 500,800 \text{ cal mole}^{-1} (\text{C}_3) \quad (3)$$

$$\Delta H_{\text{subl}}^{\circ} = 3\Delta H_{\text{m}}^{\circ} + \Delta H_{\text{vap}}^{\circ} \quad (4)$$

$$\Delta H_{\text{subl}}^{\circ} - \Delta H_{\text{vap}}^{\circ} = 3\Delta H_{\text{m}}^{\circ} = 414,400 \text{ cal} \quad (5)$$

$$\Delta H_{\text{m}}^{\circ} = 138,130 \text{ cal mole}^{-1} (\text{C}) \quad (6)$$

$$\Delta S_{\text{m}}^{\circ} = 36.5 \text{ cal mole}^{-1} \text{ K}^{-1} (\text{C}) \quad (7)$$

Note that the sublimation into P_3 requires 3 gram atoms of graphite; therefore, $3\Delta H_{\text{m}}$ was used in Eq. (3).

The same results for $\Delta H_{\text{m}}^{\circ}$ and $\Delta S_{\text{m}}^{\circ}$ were obtained by plotting $\ln P_1$ versus T^{-1} for the monatomic gaseous carbon because each gaseous species is in equilibrium with all other species as well as with the coexisting condensed phase. The results show that the standard enthalpy of melting per gram atom of C is 1.6 times as large as the standard enthalpy of vaporization per mole of C_3 , in contradiction to the energetics and molecular concepts of phase transitions. Such large values of the enthalpy and the entropy of fusion have never been encountered in melting pure elements (Refs. 13 and 14). The standard entropy of fusion of the metallic elements is usually close to $2 \text{ cal mole}^{-1} \text{ K}^{-1}$ according to Richards' rule and no more than $7.5 \text{ cal mole}^{-1} \text{ K}^{-1}$ for the metalloids with the strongest covalent bonds (Ref. 13). The entropies of melting of the Carbon Group elements having a tetragonal crystal structure and close to carbon are 7.17 for silicon and 7.30 for germanium. Therefore, the entropy of melting of tetragonal carbon,

i.e., diamond, should be very close to 7.0, and since the entropy change for the diamond to graphite transformation is -1.3, the entropy of melting of graphite should be 5.7 if it were to melt at 3780 K as claimed. The entropy of melting capable of showing a detectable break as in Fig. 3 is therefore 6.4 times larger than the upper limit permitted by the entropy value. For such an entropy of melting, the break in the vapor pressure curve is indicated by the broken line on the upper left side in the liquid region. The break is gentle and cannot be determined by the usual errors encountered at temperatures above 1000 K. Likewise, for silicon, which vaporizes into Si(g), Si₂(g), and Si₃(g), such a break at the melting point is concealed well within experimental errors (Refs. 13 and 14) as shown in the insert in Fig. 4. As a consequence of the entropy limitation, the melting points of the elements cannot be determined from the vapor-pressure measurements. Experimental errors in vapor-pressure measurements above 1000 K always conceal a gentle break in the vapor-pressure curve upon melting. Therefore, the lines in Fig. 2 and the break between the lower curves in Fig. 3 are unacceptable. It is interesting to note that if a phase change involving a heat effect of 138 kcal mole⁻¹ had existed, it would have been observed by a sharp break in Schoessow's temperature-power input curves extending up to 4100 K. In Schoessow's experiments, these curves could always be reproduced by cooling and reheating the same sample, indicating that melting did not occur below 4000 K.

Haaland (Ref. 14) used a Nd laser beam, 1.06 μm in wavelength and of 400 W, focused on a pyrolytic graphite bar 1.5 mm in diameter, in a gas-pressurized chamber. The laser power density was 80 kW cm⁻². The axis of the bar was also the c-axis of pyrolytic graphite. The pressure chamber was equipped with three fused quartz windows at 45-deg intervals (the first hole for the laser beam, the second for a recording optical pyrometer, and the third for a high-speed cinematograph). The chamber was pressurized with either helium or argon. The sample was laser-heated and then taken out of the pressure chamber for visual and microscopic examination for frozen droplets of liquid carbon. These droplets were quite similar to the droplets

obtained by arc-heating both pyrolytic and ATJS graphite in the experiments of Diaconis et al. X-ray diffraction patterns of frozen droplets showed sharper diffraction lines than the original graphite and the condensed vapor. The minimum pressure for obtaining liquid carbon was found to be 107 ± 2 atm and was independent of sample size and of pressurization gas. Different diffusion rates of carbon vapor in helium and argon did not alter the observed minimum pressure; therefore, 107 atm was considered to be the triple-point pressure of graphite. A hot luminous plume of vapor or plasma obscured the sample surface; therefore, the observed temperatures of 4300 to 5400 K were not considered to be related to the triple-point temperature. The observed temperatures depended on the purity and composition of the inert gas because the gaseous impurities caused ionization.

II. EXPERIMENTAL PROCEDURE

The experimental procedure in this investigation was designed to minimize the temperature measurement errors and to permit convenient visual examination of graphite during heating. The pressure chamber is shown in Fig. 5. It was connected to a vacuum pump and a pressurization gas through appropriate connections and valves. The pressure was measured with a Bourdon gauge calibrated to approximately 1% accuracy. A graphite sample holder was used for holding a disc of pyrolytic graphite, 4×2 mm, with its c-axis perpendicular to the laser beam. This alignment was necessary because of the nearly unit emissivity of graphite perpendicular to the c-axis and the conduction of heat in the same direction as the laser beam. When the sample was arranged with the c-axis parallel to the laser beam, it was difficult to melt graphite because heat was conducted laterally and away from the thermal center of the beam. A cw HF chemical laser being studied in the Aerophysics Laboratory of The Aerospace Corporation was used as the radiation source for these experiments. The laser provided a multiline (2500- to 3000-nm wavelengths) beam at about 1400 W for sample heating. Vernier control of laser power for refined temperature control at the test samples was accomplished by means of H_2 injection rate variation. Details of the laser operation were published by Spencer et al. (Ref. 16). The HF laser beam entered through a sapphire window capable of withstanding several hundred atmospheres of pressure. The absorptivity of the window was obtained with standard sources of illumination for correct temperature readings with a disappearing filament optical pyrometer magnifying the heated zone by a factor of five. The window was tested for absorptivity after a number of experiments; in no case, were significant degrees of fogging observed. The optical pyrometer and the laser beam were aligned as parallel as possible to obtain an optical path free from soot. It was assumed that even if soot were formed during heating the laser beam would revaporize it and thus keep the optical path clear. Vapor species consisting of various polymers of carbon do not absorb radiation (Refs. 17 and 18) in the vicinity

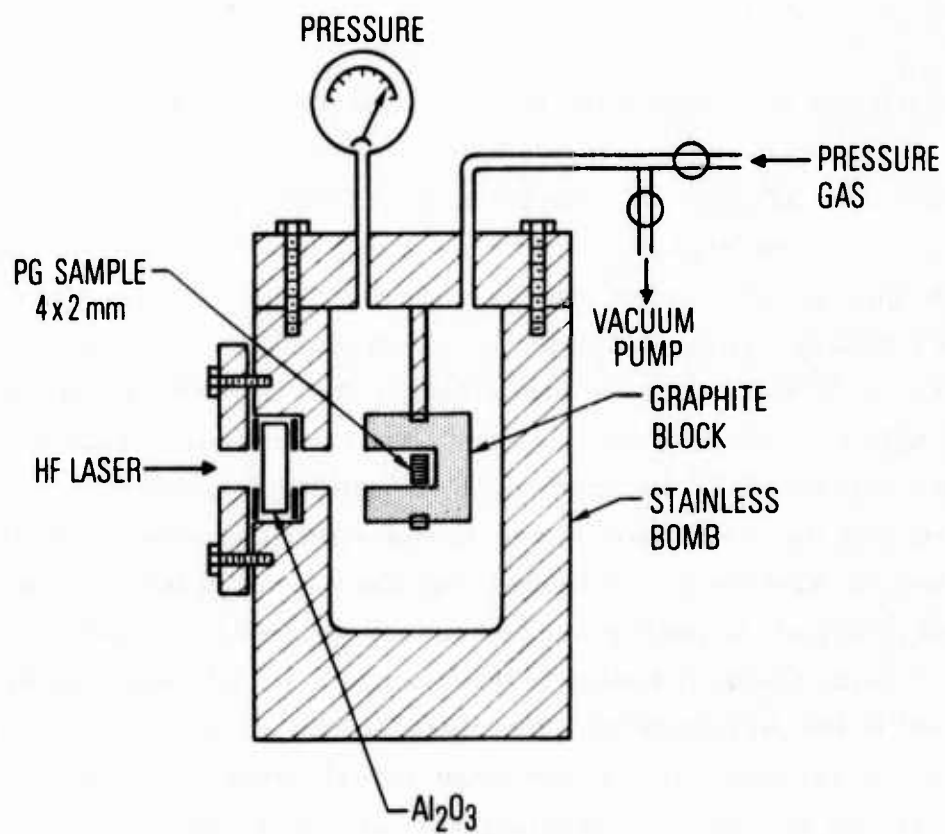


Fig. 5. Apparatus

of 656 nm wavelength for the optical pyrometer. Three Swan bands for $C_2(g)$ are accessible to the pyrometer (Ref. 18), but calculations show that they cannot cause more than 1 K error because (a) the bands are very weak (they have intensities of 1 or 2 on a scale of 10) and (b) $C_2(g)$ constitutes only 0.06 mole fraction of the carbon vapor. The laser beam was focused on an area of approximately 3 mm^2 so that the power density was about 50 kW cm^{-2} on the graphite specimen. The laser beam formed a crater or a deep valley in graphite and provided a blackbody cavity for optical temperature measurements. The emissivity of graphite perpendicular to the c-axis is 0.92 at 1200 K, increases with increasing temperature, and probably reaches unity at 4000 K (Ref. 19). In addition, solid phases generally become more emissive upon melting. A value of 0.95 instead of 1.00 for the emissivity of graphite causes an error of less than 40 K in optical temperature measurements. On the basis of these arguments, it seems justifiable to neglect the emissivity correction to the optical temperature measurements in this investigation

An experimental run was conducted as follows: The chamber was evacuated and flushed with the pressurization gas, and this process was repeated to purge the system and to remove adsorbed gases from graphite. The optical pyrometer and the laser beam were aligned on the target; then the pressure chamber was positioned and pressurized with pure argon, neon, or krypton. The pyrometer was set to a selected temperature, and the laser power was increased gradually. When the temperature reached the selected point, as observed by the pyrometer, the laser was shut off. The duration of the entire heating cycle was only 5 sec. The change in pressure during heating was small. The final pressure, i.e., at the end of heating, was taken to be the equilibrium pressure over the graphite. The gas provided an effective blanket over the graphite for the equilibrium vapor pressure determination at the triple point. Equilibration of the vapor pressure of condensed phases with inert pressurization gases as effective blankets has been used as an established technique for the measurements of vapor pressure (Refs. 20 and 21). After the laser heating, the chamber was depressurized and the graphite disc was taken out and examined under a microscope at 50 \times magnification. When the pressure was above 120 atm and the temperature above 4130 K, a

small frozen droplet of graphite was observed. The higher the pressure, the larger the size of frozen droplet for a given temperature. At pressures below 120 atm, liquid droplets were never observed. A number of runs with helium were unsuccessful because the laser beam in helium appeared to vacillate, usually by moving up and down. A total of 109 successful runs were made with neon, argon, and krypton; 47 of which showed the existence of liquid.

A. PHASE EQUILIBRIA RESULTS

The results for phase equilibria are presented in a phase diagram (Fig. 6), where it is shown that the triple point of graphite is 120 ± 10 atm and 4130 ± 30 K. Numerous experiments at 2-atm increments of pressure from 105 to 125 atm were carried out at various temperatures to ascertain the triple-point pressure. No liquid was observed when the pressure was less than 120 atm; this pressure was therefore the equilibrium vapor pressure of the coexisting liquid and solid phases. The line for the melting temperature of graphite as a function of pressure is nearly vertical with a slope of 27 atm K^{-1} according to previous investigations at pressures much higher than those of this investigation (Refs. 1, 2, 4, 5, and 8), as will be discussed later. This line separates the samples containing the frozen droplets from those without and therefore represents the melting temperatures at various pressures. The phase boundary curves for solid-vapor and liquid-vapor equilibria are also shown in Fig. 6, as will be discussed later in detail.

B. MICROSTRUCTURE

A number of samples have been examined under a microscope by ordinary and cross-polarized light, and a scanning electron microscope (SEM) to obtain the structures of various types of graphite in the sample after laser heating. Figure 7 is an SEM micrograph of Sample No. 152 containing a droplet of frozen liquid approximately 0.4 mm in size. This sample was heated to 4140 K under 146 atm of neon. Figure 8 is a photomicrograph of the same sample under ordinary light, which shows that the droplet is very shiny, whereas the background is dull black. Figures 9 and 10 show Sample No. 140 at 4180 K and 143 atm of neon. The frozen liquid, nearly 2 mm long,

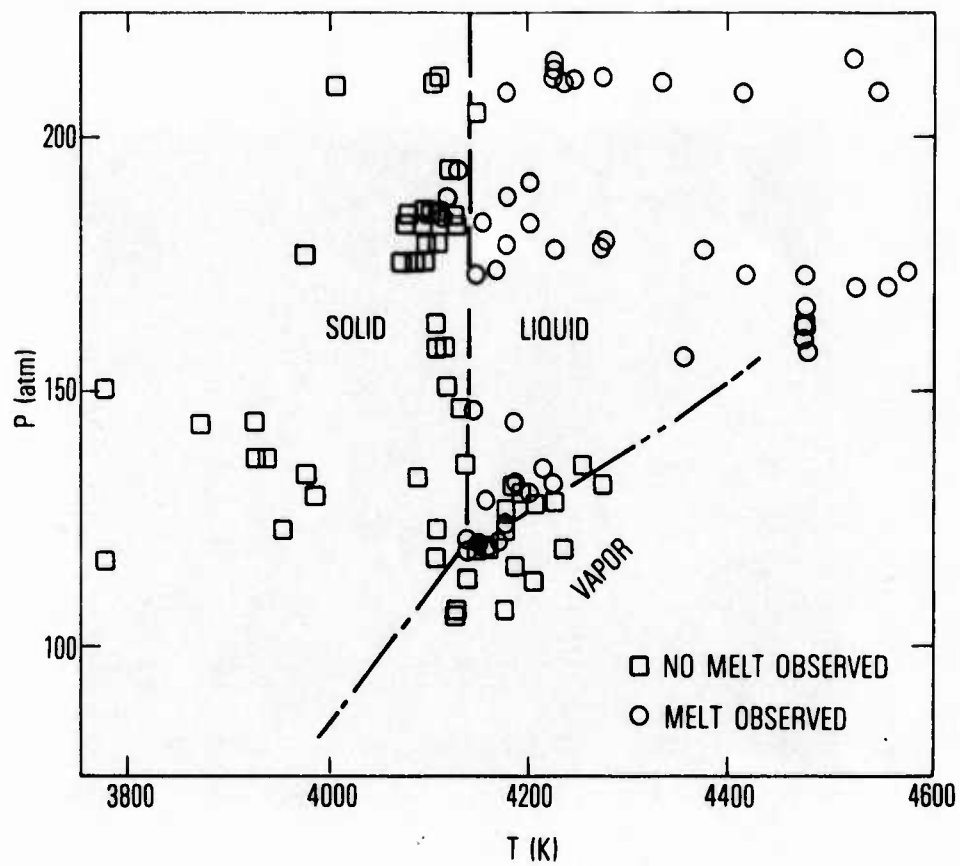


Fig. 6. Graphite-liquid-vapor triple point and melting temperatures of graphite.

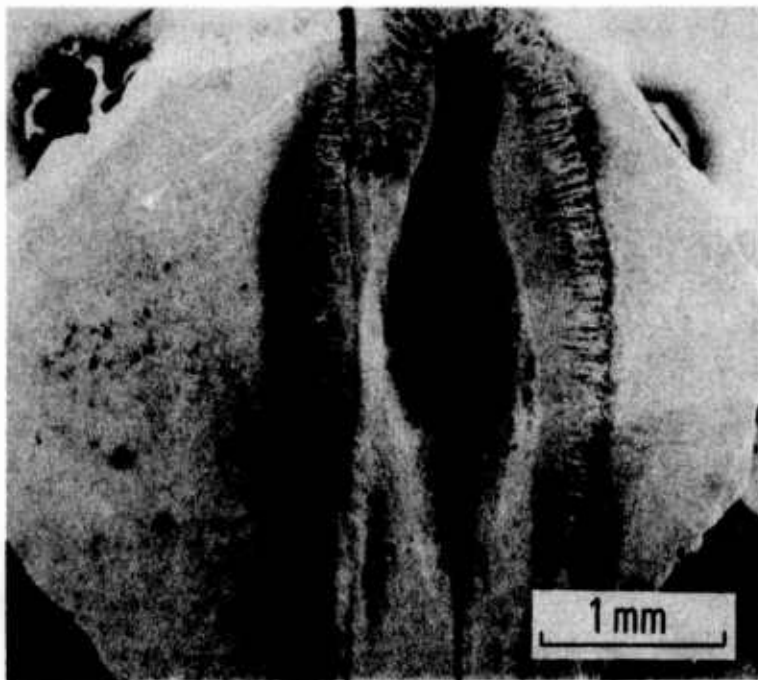


Fig. 7. Sample No. 152 at 4140 K and 146 atm of neon.
(Electron micrograph. Liquid droplet is in
center.)

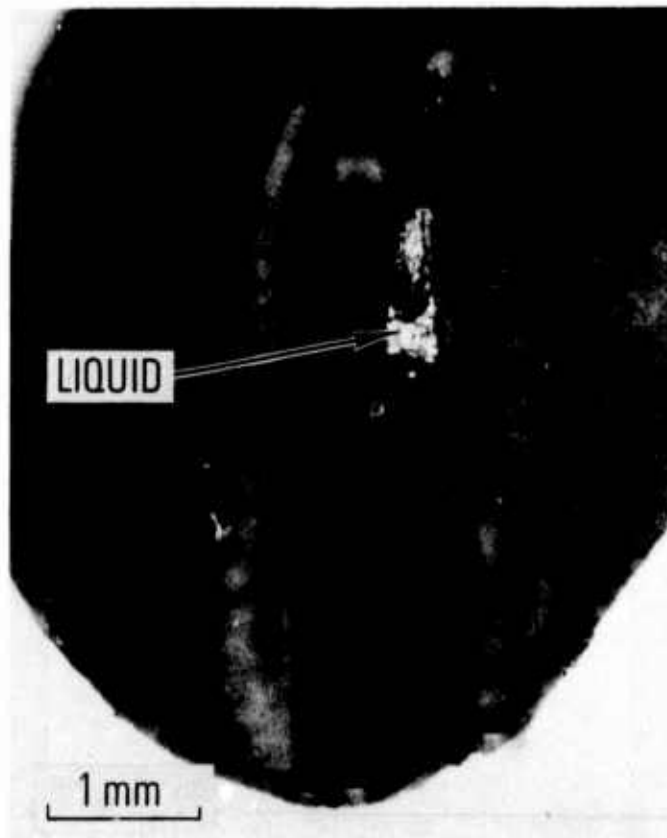


Fig. 8. Same as Fig. 7. (Photomicrograph with ordinary light. Note that liquid is very shiny and unaltered graphite is very dull dark gray.)

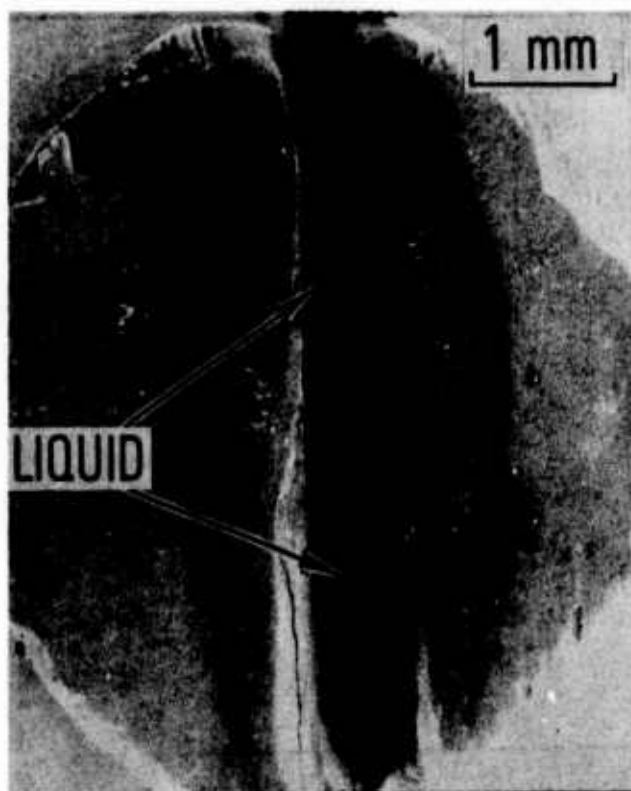


Fig. 9. Sample No. 140 at 4180 K and 143 atm of neon.
(Electron micrograph. Liquid is in center.)



Fig. 10. Same as Fig. 9. (Photomicrograph with ordinary light. Liquid is shiny and close to 2 mm in length.)

was in one piece when it was taken out of the pressure chamber, but it was split inadvertently by handling. An unusually well-defined liquid droplet was obtained at 4475 K and 160 atm of neon in Sample No. 11, as shown in the photomicrograph (Fig. 11). This sample was split, and an SEM micrograph of the droplet perpendicular to the direction in Fig. 11 was taken (Fig. 12). Figure 13 is an SEM micrograph of the central portion of the droplet; where the platelets of frozen liquid are clearly depicted. This portion of the split sample was subsequently mounted, polished, and photographed under cross-polarized light and at various angles (Figs. 14-18). Figure 19 is a photograph (original in color) of the droplet under cross-polarized light with a red-sensitive tint that shows well-defined platelets of frozen liquid. The structure of the frozen liquid is distinct from the pyrolytic graphite matrix, i.e., it is crystalline, acicular, and platelike in appearance. Underneath the frozen liquid droplet, the laminae of pyrolytic graphite were welded, and desorbed gases were trapped as shown in Figs. 14-18. The photomicrographs of the droplet in Sample No. 152 (Fig. 7) showed identical structures and are therefore not presented in this report. Figure 20 is a photomicrograph under cross-polarized light that shows the fluffy condensate on the outer edge of the crater in Sample No. 11.

Figure 21 is a photograph of Sample No. 32 heated to 4005 K under 210 atm of neon. This sample was mounted, progressively ground and polished across the crater, and photomicrographed under cross-polarized light (Figs. 22-25). It is clear that no significant structural change occurred in this sample because of heating. Sample No. 38 (Figs. 26-31) is similar to Sample No. 32, but it was heated to 4120 K in 193 atm of krypton. The crater is considerably deeper than that in Fig. 21 because the temperature was higher. The surface of the crater has a uniform structure and is dull black. Near the outer edges, the condensed vapor affected the appearance of graphite. Figure 28 is an SEM micrograph of the central portion of Fig. 27 just below the large crack. The outer left side edge of the crater in Fig. 26 is shown at a higher magnification in Fig. 29. Nodular condensed particles of soot can be seen over tightly packed sheets of pyrolytic graphite. A composite



Fig. 11. Sample No. 11 at 4475 K and 160 atm of neon. (Photomicrograph with ordinary light. Liquid is at lower left.)

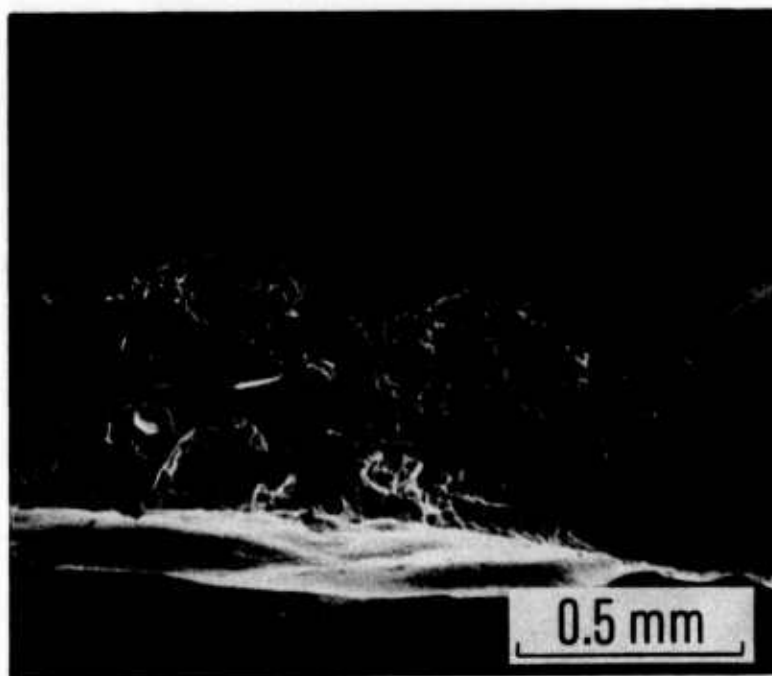


Fig. 12. Cross section of Sample No. 11. (Electron micrograph. Lateral view, perpendicular to Fig. 11 after sample was split. Liquid is in center against dark dull gray background.)

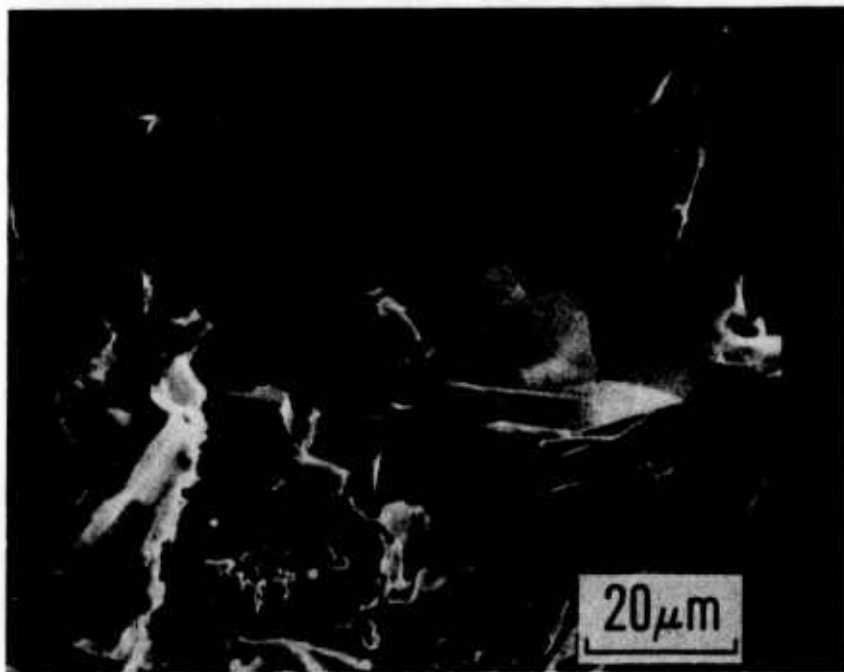


Fig. 13. Same as Fig. 12. (Structure of frozen liquid droplet in center)

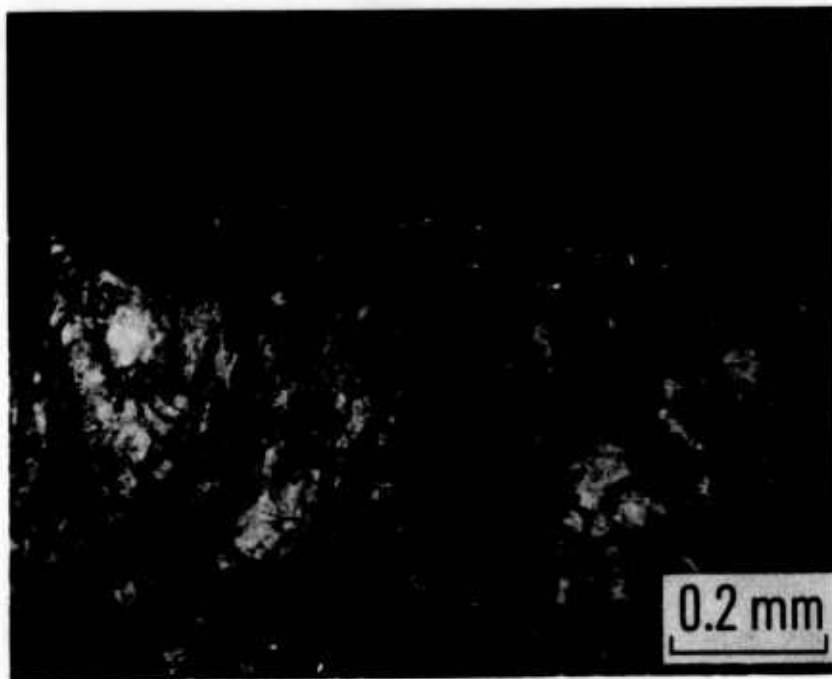


Fig. 14. For caption, see Fig. 18.

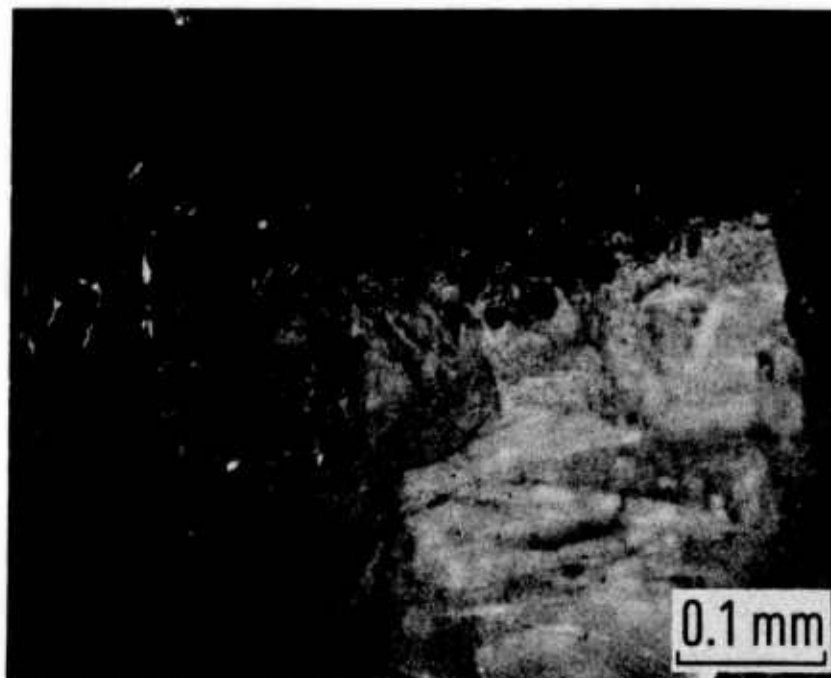


Fig. 15. For caption, see Fig. 18.

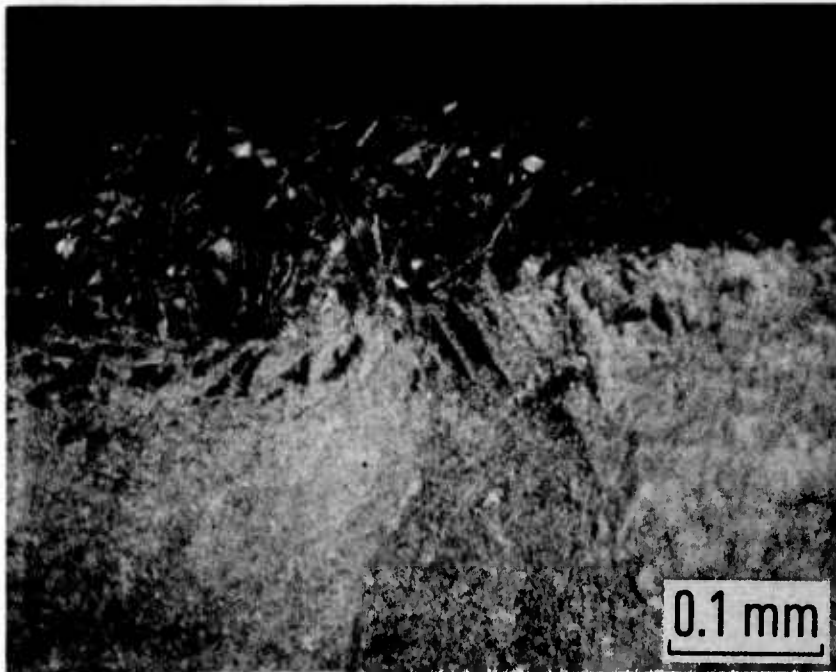


Fig. 16. For caption, see Fig. 18.

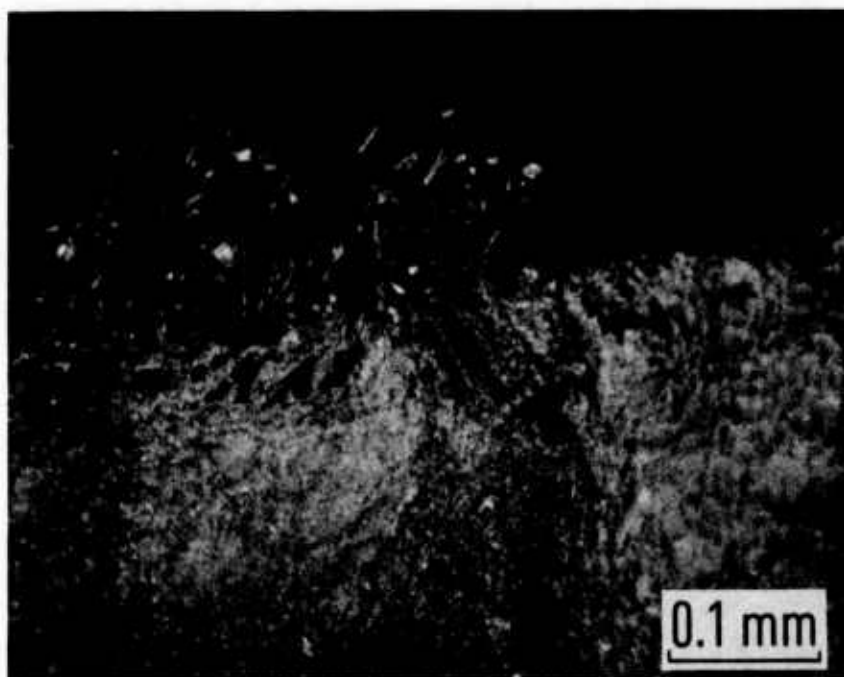


Fig. 17. For caption, see Fig. 18.

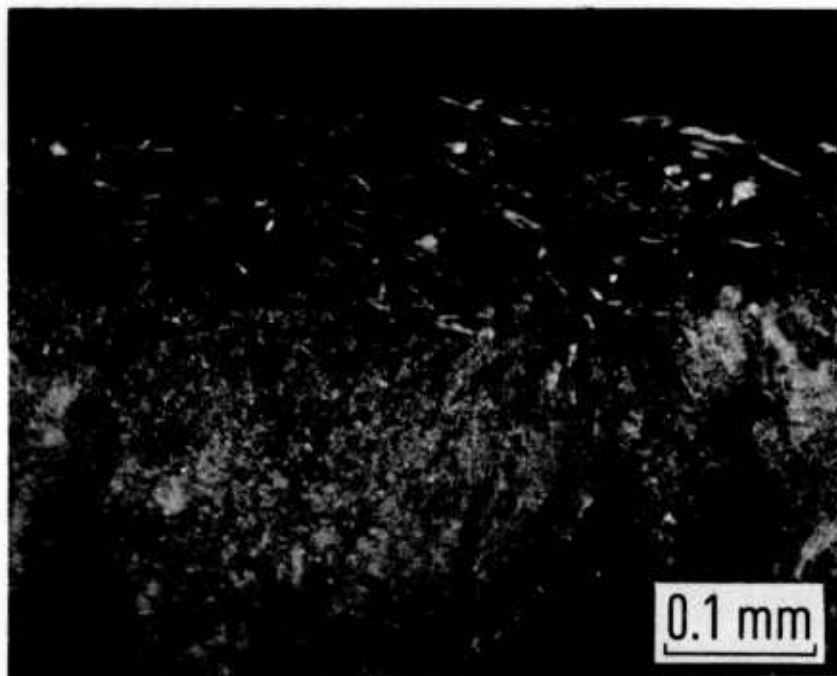


Fig. 18. Cross section of Sample No. 11 under polarized light at various angles. (Polishing with diamond powder or with alumina shows no detectable difference in micrographs.)



Fig. 19. Sample No. 11, frozen droplet, cross-polarized light, red-sensitive tint.
(Original in color)

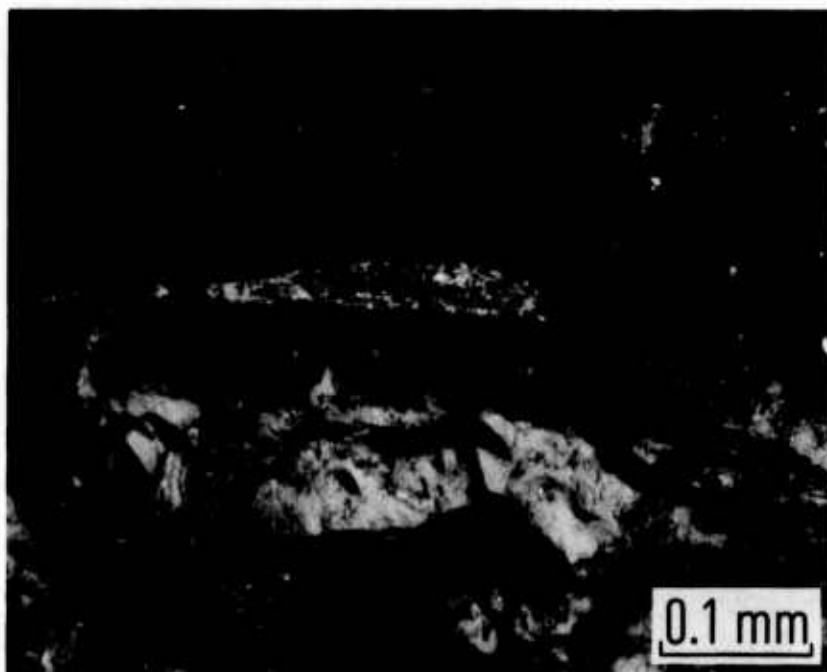


Fig. 20. Sample No. 11. (Edge of crater showing condensate under cross-polarized light.)

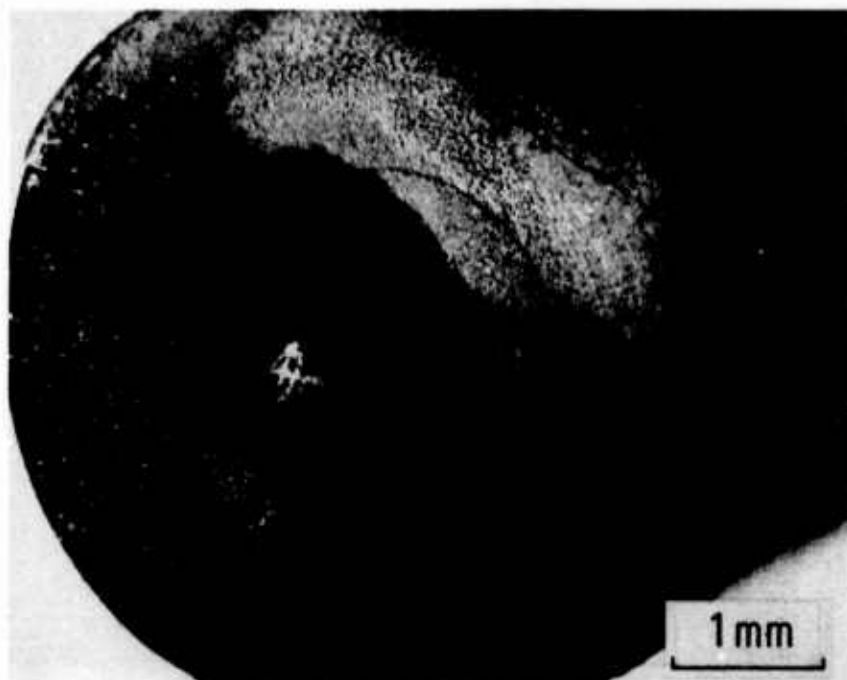


Fig. 21. Sample No. 32 at 4005 K and 210 atm of neon.
(Photomicrograph with ordinary light.)

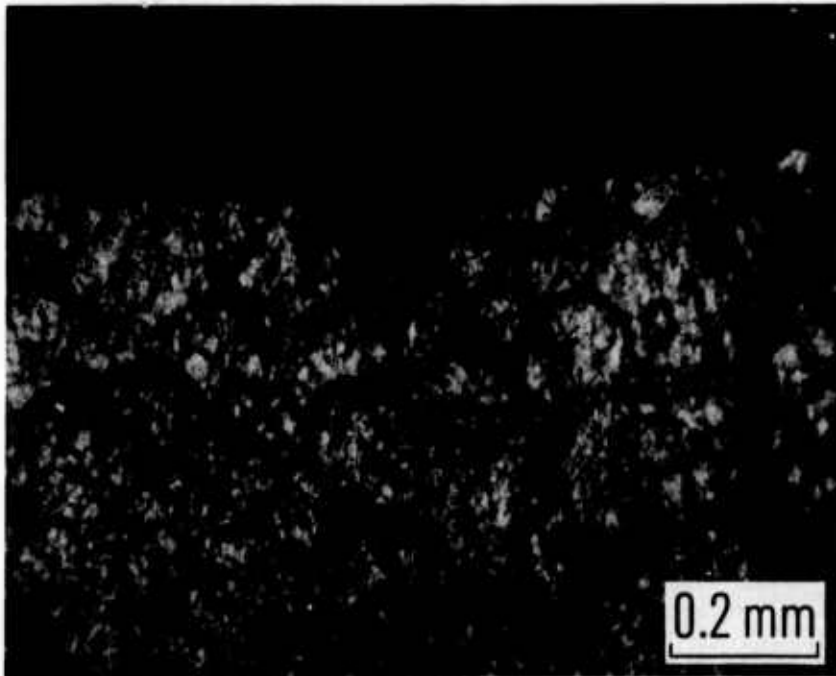


Fig. 22. For caption, see Fig. 25.



Fig. 23. For caption, see Fig. 25.

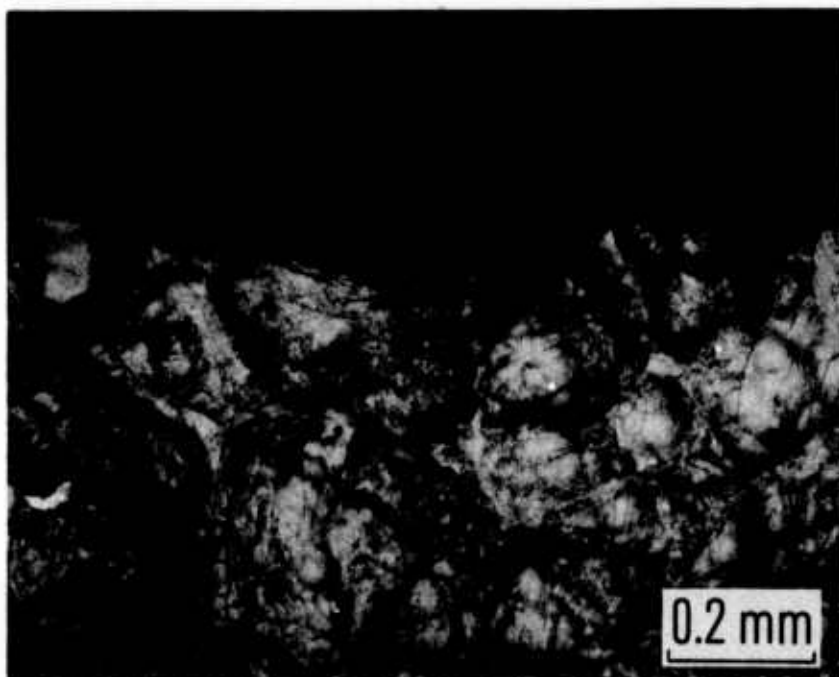


Fig. 24. For caption, see Fig. 25.

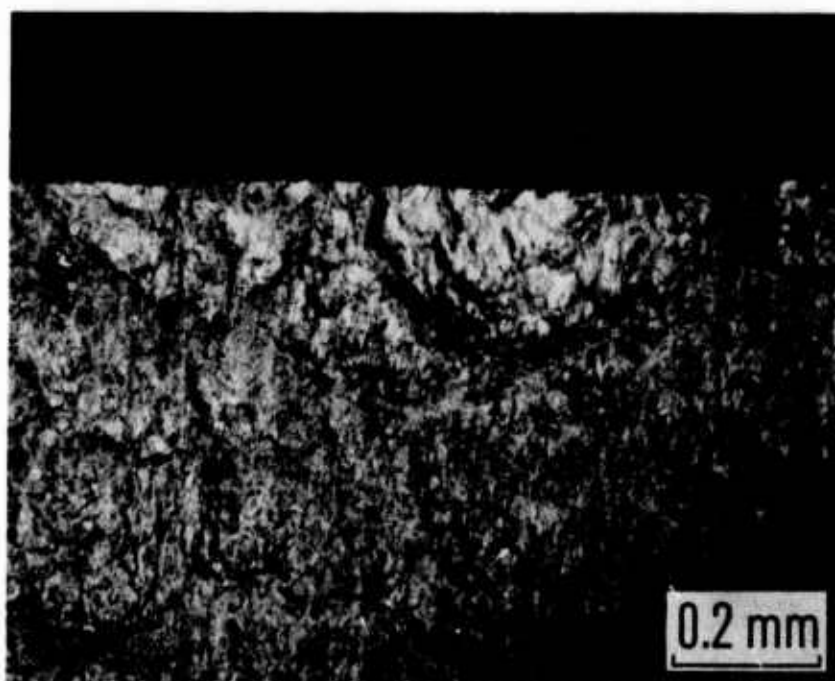


Fig. 25. Sample No. 32 showing no liquid. (Crater, ground and polished progressively from lower left in Fig. 21 to upper right. Cross-polarized light)

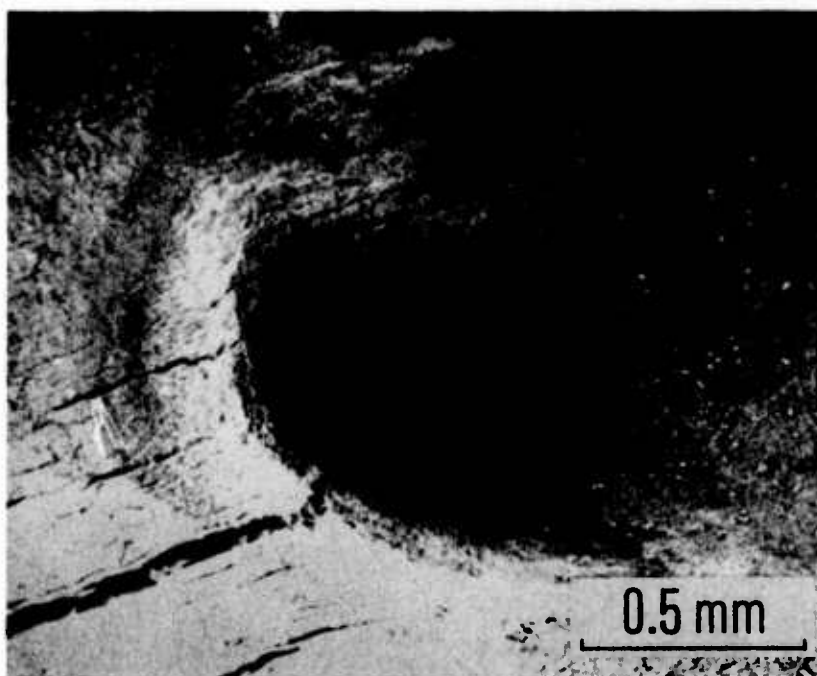


Fig. 26. Sample No. 38 at 4120 K and 193 atm of krypton. (Electron micrograph)

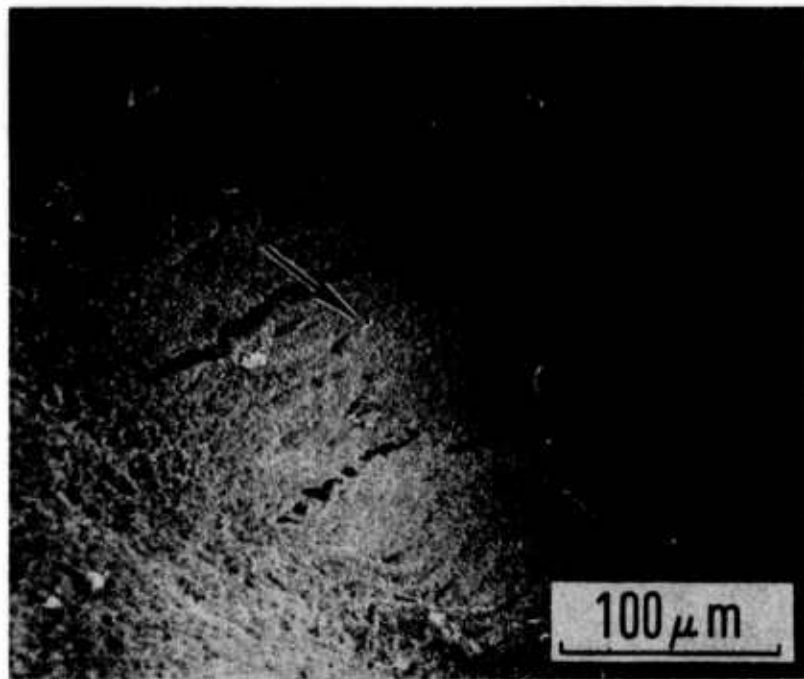


Fig. 27. Same as Fig. 26. (Upper central part of crater)

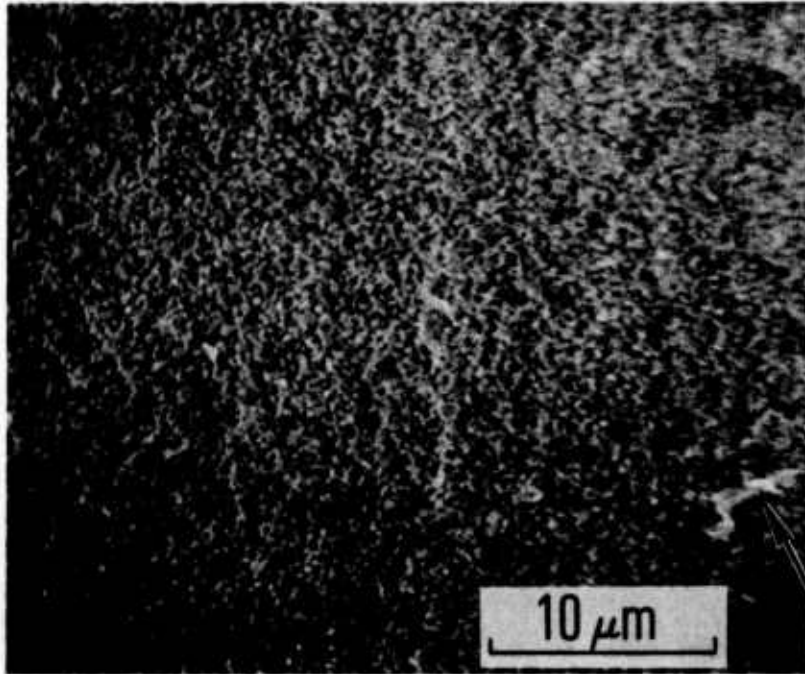


Fig. 28. Central part of Fig. 26, just below crack.



Fig. 29. Outer edge of crater in Fig. 26.



Fig. 30. For caption, see Fig. 31.



Figure 31. View of Sample No. 38 from right side of Fig. 29 to central crack in Fig. 27. (Right side of Fig. 30 matching left side of Fig. 31 is marked.)

micrograph of Fig. 27 at 3000 \times , in the vicinity of the crack is shown in Figs. 30 and 31. Again, these micrographs confirm that there is no significant structural change in graphite when the liquid phase is absent.

The micrographs of frozen liquid graphite (Figs. 11-19) are quite similar to those of frozen liquid obtained by Diaconis et al. (Ref. 9). In their experiments, pyrolytic graphite and ATJS graphite melted by arc heating, and ATS graphite melted by resistance-heating yielded frozen droplets having an identical microstructure. Photomicrographic evidence similar to Figs. 11 and 14 were also obtained recently by Haaland (Ref. 15).

C. X-RAY AND ION MICROPROBE MASS ANALYSES

Sample No. 140 was subjected to x-ray analysis at four locations.

- (1) At the outside of the graphite disc far away from the crater, the x-ray pattern lacked back reflections, which is typical of pyrolytic graphite.
- (2) The fluffy condensate on the ridge of the crater gave a weak pattern and broad and diffuse back-reflection lines of low intensity. The lattice parameter was that of crystalline graphite.
- (3) Inside the crater and away from the melt, the material behaved as natural graphite, but the diffraction lines were not as sharp as those of frozen melt.
- (4) The frozen graphite gave very sharp diffraction lines all the way out into the deep back-reflection region indicating that important structural changes had occurred by melting. A similar contrast was observed by Haaland (Ref. 15).

Selected locations in Sample No. 11, identical with those in Sample 140, were subjected to ion microprobe mass analysis with O_2^+ bombardment at 20 kV and 1 nA. The spectra of secondary ions were examined and recorded as intensity versus mass number. The results are summarized as follows:

- (1) The outer portion away from the crater showed a strong peak for C_1^- and a very weak peak for C_2^- .
- (2) The fluffy condensate gave stronger peaks of C_1^- and C_2^- and a weak peak for CH^- , C_1^- being the strongest peak.
- (3) Inside the crater half way between the edge and the center, the peaks were similar to those for pyrolytic graphite but stronger in intensity.
- (4) The frozen liquid gave the following peaks with their intensities in parentheses: (C_1^- (strong),

CH^- (very weak), C_2^- (very strong), C_3^- and C_4^- (strong), C_5^- and C_6^- (medium), C_7^- and C_8^- (weak), and C_9^- and C_{10}^- (very weak). None of the spectra indicated the presence of such impurities as Si, Ca, Ti, Zr, Fe, and Cu; the peak for CH^- might be due to moisture or adsorbed hydrogen. The results showed that (1) there was no segregation of impurities because of heating, evaporation, or melting, (2) the frozen droplets gave sharp peaks, characteristic of graphite having a high degree of crystalline perfection, and (3) the spectra for the areas of crater away from the frozen droplet were quite different from the spectra for the droplet.

III. DISCUSSIONS

A. TRIPLE-POINT PRESSURE

The measurements of vapor pressure over solid or liquid graphite do not present unusual difficulties. In general, if the pressurization gas is not greatly disturbed during heating, or a cavity provides a reasonably static volume, the equilibrium vapor pressure can be equated to the inert gas pressure (Ref. 19). The results based on this procedure for the triple-point pressure and obtained by Basset, Jones, Noda, and Vereshchagin, and Fateeva are 102, 100, 110-120, and 100 atm, respectively. Horizontal graphite bars having a central cavity and heated by electric resistance, as in the experiments of Diaconis et al., had a triple-point pressure of 102 atm, whereas graphite discs heated by electric arc encountered a great deal of gas-phase perturbation near the surface so that 135 atm was the minimum pressure at which the liquid phase was formed. The specimens used by Schoessow and Diaconis et al. (Fig. 1) and those with central cavities used by Jones also provided reasonably static conditions for equilibrating the pressurization gas with the graphite vapor. It is believed that the triple point obtained by the authors, i. e., 120 atm, is in reasonable agreement with the previously published values obtained experimentally under widely different experimental conditions.

The experimental values of the vapor pressure of solid graphite can be extrapolated to the triple point for comparison. The upper temperature limit for the vapor pressure measurements is about 3000 K for the effusion experiments (Refs. 22, 23, and 24); although for the Langmuir experiments, higher temperatures have been attained. Because of very small evaporation coefficients for dimeric and polymeric gaseous carbon species, the Langmuir method cannot give reliable data. Extrapolation of the best equilibrium measurements to 4130 K yields 3.80 atm, and to 4760 K, 103 atm, as recommended by Leider, Krikorian, and Young (Ref. 24). The JANAF Tables (Ref. 13) give a little lower values (Fig. 3), whereas Palmer Shelef

(Ref. 10) recommend a little higher values. It is believed that the vapor pressure measurements are high at low temperatures because of desorption of gases from graphite and low at high temperatures because of low evaporation coefficients for various vapor species. Published results in the range of 2000 to 3000 K differ by more than an order of magnitude. It is therefore not surprising that the extrapolated values of pressure to the triple point are low. An error of 600 K in the measurements of the triple point could account for the discrepancy, but the experimental technique used by the authors, as well as by Schoessow and by Diaconis et al., cannot permit an error of this magnitude.

B. TRIPLE-POINT TEMPERATURE

The measurements of the triple-point temperature are much more difficult than the triple-point pressure. Interference from soot, wavering images of heated zones caused by gas circulation, nonuniformity of temperature, and emissivity contribute to the uncertainties in ordinary monochromatic optical temperature measurements. The two-color pyrometry used by Fateeva et al. required large corrections. The agreement between direct and indirect measurements of temperature in the experiments of Schoessow indicates that a properly designed apparatus can minimize these errors. Electrical resistance heating produces lower temperatures on the surface because of the radiative heat loss; therefore, the interior of a bar is always hotter than the surface. Consequently, the triple-point temperatures reported by Basset and Noda are probably low, possibly by 100 K. Jones, Schoessow, and Diaconis et al. minimized temperature nonuniformity by sighting on a cavity in which the heat loss was minimal and the blackbody conditions were achieved. The emissivity is not a serious problem except when the a-b surface (the plane of densest atomic population) is heated as discussed by Diaconis et al. It is believed that the laser heating, as used in this investigation, eliminates the error resulting from the radiative heat loss and also minimizes the soot interference in the temperature measurements. A plasma observed by Haaland during Nd laser heating was

absent in the authors' experiments. The triple points determined by Basset, Jones, Noda, Schoessow, Vereshchagin and Fateeva, and Diaconis et al. are 4000, 4030, 4020, 4300, 4040, and 4200 K, respectively; the average is 4100. The present result, i.e., 4130 ± 30 K, is in close agreement with the average and lies in the range of 4100 to 4300 reported by Diaconis et al.

C. PHASE DIAGRAM

The solid-liquid phase boundary in Fig. 6 is based on the experimental data. The pressure range in this investigation is not large enough to determine the slope of the boundary line; a slope of 27 atm K^{-1} is based on the average of published values (Refs. 1, 2, 4, 5, and 8) at sufficiently high ranges of pressure. The liquid-vapor and solid-vapor boundaries are estimated and drawn within the limits imposed by the data and the requirement for the entropies of phase changes. Accurate measurements of the vapor pressure in the range 3000 to 4000 K are necessary for reliable representation of the solid-vapor boundary curve. Laser heating a sample suspended from a thermogravimetric balance could provide the required data, on the basis of the method of Baur and Brunner (Ref. 21).

IV. SUMMARY

A technique was developed for determining the graphite-liquid-vapor triple point and melting temperatures of graphite by an HF laser beam in the range 120 to 215 atm. The results showed that (1) the triple point was 120 ± 10 atm and 4130 ± 30 K, (2) the melting temperature was nearly independent of pressure up to 215 atm, and (3) a phase diagram could be drawn in the vicinity of 4100 K (Fig. 6). The pressure-dependence of melting, based on published results, was selected to be 27 atm K^{-1} .

A critical review of relevant investigations on the triplet point and on the melting temperatures was made and compared with the present investigation.

A thorough examination of the frozen liquid droplets, the laser-formed craters, the condensed vapor, and the pyrolytic graphite matrix was made by photomicrography, scanning electron micrography, x-ray diffraction, and ion microprobe mass analysis. The results showed that the frozen droplets were pure and distinctly well-defined in structure.

REFERENCES

1. J. Basset, J. Phys. Radium 10, 217 (1939).
2. M. T. Jones, Summary Report PRC-3, National Carbon Research Laboratories, Parma, Ohio (1958).
3. T. Noda, Proceedings of an International Symposium on High Temperature Technology, McGraw-Hill Book Co., Inc., New York (1960).
4. F. P. Bundy, J. Chem. Phys. 38, 618 (1963).
5. N. S. Fateeva, L. F. Vereshchagin, and V. S. Kolotygin, Physics-Doklady 8, 893 (1964).
6. L. F. Vereshchagin and N. S. Fateeva, Soviet Physics, JETP 28, 597 (1969).
7. N. S. Fateeva and L. F. Vereshchagin, JETP Letters 13, 110 (1971).
8. G. J. Schoessow, Phys. Rev. Letters 21, 738 (1968); for details see Report NASA CR-1148, NASA, Washington, D.C. (July 1968).
9. N. S. Diaconis, E. R. Stover, J. Hook, and G. F. Catalano, Graphite Melting Behavior, AFML-TR-71-119, Air Force Materials Laboratory, Wright-Patterson Air Force Base, Ohio (July 1971).
10. H. B. Palmer and M. Shelef, "Vaporization of Carbon," in Chemistry and Physics of Carbon, ed., P. L. Walker, Jr., Marcel Dekker, Inc., New York (1968).
11. A. G. Whittaker, P. L. Kintner, L. S. Nelson, and N. Richardson, 12th Biennial Conference on Carbon, Extended Abstracts and Program, American Carbon Society and School of Engineering, University of Pittsburgh, Pittsburgh, Pennsylvania, 28 July - 1 August 1975.
12. D. R. Stull and H. Prophet, JANAF Thermochemical Tables, Superintendent of Documents, U.S. Government Printing Office, Washington, D.C. (1971).
13. N. A. Gokcen, Thermodynamics, Techscience, Inc., Hawthorne, California (1975), Chapter V.

14. R. Hultgren, R. L. Orr, and K. K. Kelley, Selected Values of Thermodynamic Properties of Metals and Alloys, John Wiley and Sons, Inc., New York (1963).
15. D. Haaland, Ref. 11, p. 51.
16. D. J. Spencer, H. Mirels, and D. A. Durran, "Performance of CW HF Chemical Laser with N₂ or He Diluent," J. Appl. Phys., 43 1151 (1972).
17. E. L. Lee and R. H. Sanborn, High Temp. Sci. 5, 438 (1973).
R. H. Sanborn, J. Chem. Phys. 49, 4219 (1968).
18. L. Gausset, G. Herzberg, A. Lagerquist and B. Rosen, Disc. Faraday Soc. 35, 113 (1963); R. W. B. Pearse and A. G. Gaydon, The Identification of Molecular Spectra, John Wiley and Sons, New York (1963), p. 95.
19. Pyrolytic Graphite Handbook, Metallurgical Products Department, General Electric Co., Schenectady, New York (1964).
20. G. Gatlow and A. Schneider, Angew. Chem. 71, 189 (1959).
21. E. Baur and R. Brunner, Helv. Chim. Acta 17, 958 (1934).
22. T. A. Milne, J. A. Beachey, and F. T. Greene, AFML-TR-71-182, Air Force Materials Laboratories, Wright-Patterson Air Force Base, Ohio (September 1971).
23. P. D. Zavitsanos and G. A. Carlson, SC-CR-70-6126, Sandia Laboratories, Albuquerque, New Mexico (September 1972).
24. H. R. Leider, O. H. Krikorian, and D. A. Young, Carbon 11, 555 (1973).

LABORATORY OPERATIONS

The Laboratory Operations of The Aerospace Corporation is conducting experimental and theoretical investigations necessary for the evaluation and application of scientific advances to new military concepts and systems. Versatility and flexibility have been developed to a high degree by the laboratory personnel in dealing with the many problems encountered in the nation's rapidly developing space and missile systems. Expertise in the latest scientific developments is vital to the accomplishment of tasks related to these problems. The laboratories that contribute to this research are:

Aerophysics Laboratory: Launch and reentry aerodynamics, heat transfer, reentry physics, chemical kinetics, structural mechanics, flight dynamics, atmospheric pollution, and high-power gas lasers.

Chemistry and Physics Laboratory: Atmospheric reactions and atmospheric optics, chemical reactions in polluted atmospheres, chemical reactions of excited species in rocket plumes, chemical thermodynamics, plasma and laser-induced reactions, laser chemistry, propulsion chemistry, space vacuum and radiation effects on materials, lubrication and surface phenomena, photo-sensitive materials and sensors, high precision laser ranging, and the application of physics and chemistry to problems of law enforcement and biomedicine.

Electronics Research Laboratory: Electromagnetic theory, devices, and propagation phenomena, including plasma electromagnetics; quantum electronics, lasers, and electro-optics; communication sciences, applied electronics, semiconducting, superconducting, and crystal device physics, optical and acoustical imaging; atmospheric pollution; millimeter wave and far-infrared technology.

Materials Sciences Laboratory: Development of new materials; metal matrix composites and new forms of carbon; test and evaluation of graphite and ceramics in reentry; spacecraft materials and electronic components in nuclear weapons environment; application of fracture mechanics to stress corrosion and fatigue-induced fractures in structural metals.

Space Physics Laboratory: Atmospheric and ionospheric physics, radiation from the atmosphere, density and composition of the atmosphere, aurorae and airglow; magnetospheric physics, cosmic rays, generation and propagation of plasma waves in the magnetosphere; solar physics, studies of solar magnetic fields; space astronomy, x-ray astronomy; the effects of nuclear explosions, magnetic storms, and solar activity on the earth's atmosphere, ionosphere, and magnetosphere; the effects of optical, electromagnetic, and particulate radiations in space on space systems.

THE AEROSPACE CORPORATION
El Segundo, California